URSI GASS 2020, Rome, Italy, 29 August - 5 September 2020

Electrode-based implanted HBC channel characterization and SAR analysis

Q. Wang, X. Du, T. Bauer, M. Baerhold, D. Plettemeier
Chair for RF and Photonics Engineering, Communication Laboratory
Dresden University of Technology, Dresden, Germany

Abstract

This summary paper investigates the transmission channel gain and the specific absorption rate (SAR) for implanted HBC based on the galvanic-coupled implantable electrodes, to explore the suitability of human body tissue for a galvanic implanted HBC wireless communication. Based on numerical simulation and phantom measurement, the influence of the electrode length and inter-electrode distance on the channel gain and SAR has been studied. In the HBC frequency range of interest of 5MHz-50MHz, the frequency doesn't have a noticeable effect on the channel gain. Channel transmission characteristics for different distance have been shown to be similar for different electrode dimensions. With larger transmission distance, the channel gain is decreasing. Larger implanted electrode demonstrates the relative better channel gain as well as lower localized SAR peak.

1 Introduction

HBC, as a novel rising transmission technique using the conductive properties of the human body for electrical signal transfer [1], has been recently finding its potential way in the implanted wireless communication investigation for medical data transmission. The main advantage of this technology is its very small power requirement and the absence of antenna, which makes it a potential alternative scheme of wireless radio frequency communication. For implanted HBC, a pair of electrodes is used to build up an electric field that propagates through the human body, reaching a second pair of electrodes via the galvanic coupling. This study focuses on the investigation of the transmission channel gain and the SAR analysis for implanted HBC based on the galvanic-coupled implantable electrodes.

Several channel-modeling techniques have been reported to model the human body as a channel, which shows various useful aspects of HBC. Some of these techniques include four-terminal circuit model [2], finite-element approach [3], near-field electromagnetic model, and quasi-static electromagnetic models [4]. In this paper, we present the channel gain first in simulation with the commercial CST Studio Suite as a quasi-electrostatic approximation, since the dimension of the numerical model is much smaller than the wavelength of the frequency range considered. The signal excitation is in the frequency range of interest between 5MHz and 50MHz. Then the channel gain is measured in phantom via the connection of balanced balun and network analyzer. The SAR for the implanted electrodes is of significance to ensure the human safety particularly for the implanted scenarios. The effect of electrode size on the induced local peak 10-g averaged SAR will be investigated based on the simulation on human torso CAD model and Voxel model.

2 Channel gain characterization

The differential electrodes are used to couple the alternating current into the human tissue. In order to investigate the influence of the electrode size on the resulting implanted channel gain, four versions of electrode prototypes (labeled with m1, m2, m3 and m4) are proposed as shown in Figure 1. They are designed as two small cylinder electrodes placed on a dielectric rod, with correspond to two different inter-electrode distance (dielectric rod lengths) and two different conductive metal electrode lengths (cylinder copper). The diameters of the electrode part are 0.6cm. The dielectric rod part is designed to separate the differential electrodes, which can accommodate the implanted electronic components in implant transceiver.

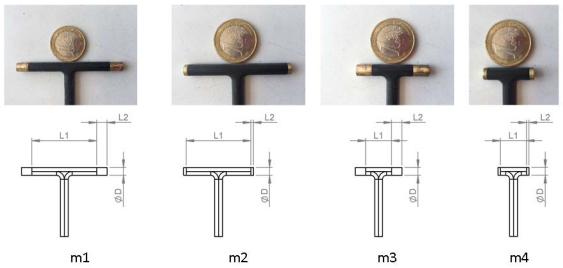

m1: L1=5cm (long rod), L2=0.8cm (long electrode)
m2: L1=5cm (long rod), L2=0.2cm (short electrode)
m3: L1=2cm (short rod), L2=0.8cm (long electrode)
m4: L1=2cm (short rod), L2=0.2cm (short electrode)

Figure 1. Fabricated electrode prototypes

Simulations of the implanted electrode-electrode transmission have been conducted using the low frequency (LF) time domain Electro-Quasi-Static (EQS) solver of CST. Four versions of electrode pairs are simulated in homogeneous human model with same differential potential excitation. The channel gain is calculated as:

$$Gain[dB] = 20 * \log_{10} \frac{|U_{RX1} - U_{RX2}|}{|U_{TX1} - U_{TX2}|}$$

Figure 2 shows the electric potential distribution for the implanted electrode. The channel gain is measured in tissue-simulating liquid phantom with 2/3 muscle dielectric properties as shown in Figure 3. The phantom recipe is listed as well. The resulting phantom has the measured dielectric permittivity 56.05 and conductivity 0.52 S/m around 30MHz. The 4 versions of electrode have relative good matching impedance characteristics inside the phantom where the measured S11 are below -10dB within the frequency band of interests.

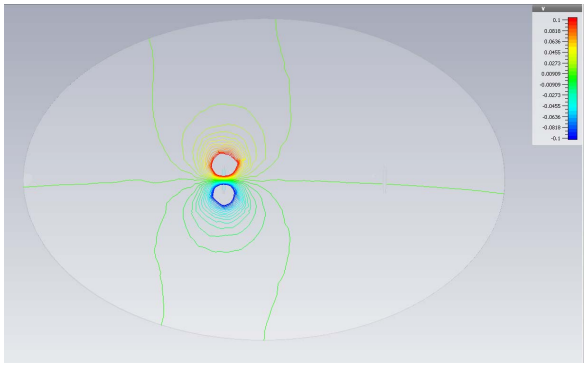

Figure 2. The electric potential distribution for the implanted electrode

Water	52.4%
NaCl	1.4%
Sugar	45%
Sodium benzoate	1.1%

Figure 3. Phantom measurement with balanced balun connection (left) and phantom recipe (right)

As shown in Figure 4, the influence of the interested frequency band 5-50MHz is not significant on channel gain, where the channel gain shows little variation for m1. The same conclusion of the approximate frequency-independent gain characteristics is drawn as well for m2, m3 and m4. With increasing transmission distance, the gain is decreasing on account of larger transmission loss.

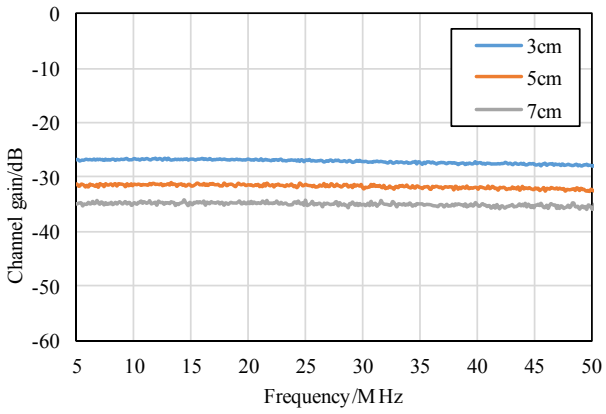

Figure 4. Measured channel gain in phantom for electrode pair m1.

The influence of the electrode length, inter-electrode distance as well as the electrode cylinder diameter on the channel gain is indicated in Figure 5, 6, 7, in which the electrode pair is aligned with each other (parallel displacement) and the distance is ranging from 3cm to 20cm.The conclusion can be summarized:

- Increasing the electrode length by 0.6cm (electrode length difference of m1 and m2) brings a channel gain enhancement of approximately 10dB;
- Increasing the inter-electrode distance by 3cm (length difference of m1 and m3) brings a channel gain enhancement of approximately 10dB;
- Increasing the electrode diameter by 0.6cm brings a channel gain enhancement of approximately 8dB.

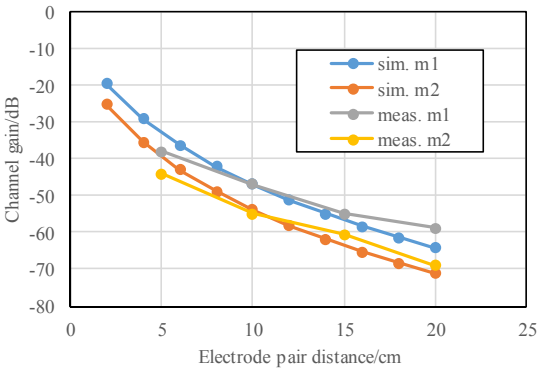

Figure 5. Electrode length influence on the channel gain
m1 (long rod and long electrode)
m2 (long rod and short electrode)

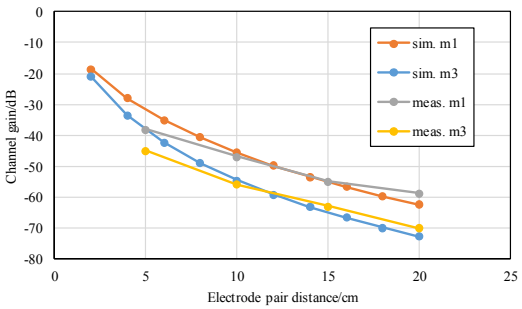

Figure 6. Inter-electrode distance influence on the channel gain
m1 (long rod and long electrode)
m3 (short rod and long electrode)

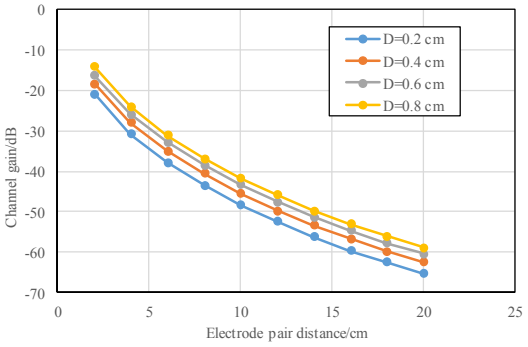

Figure 7. Simulated channel gain for sweeping electrode diameter (D), ranging from 0.2cm to 0.8cm. The fabricated prototype D is 0.6cm

Figure 8 compares the channel gain for all four versions at electrode pair distance of 5 cm. The larger electrode m1 demonstrate the relative best channel gain characteristics.

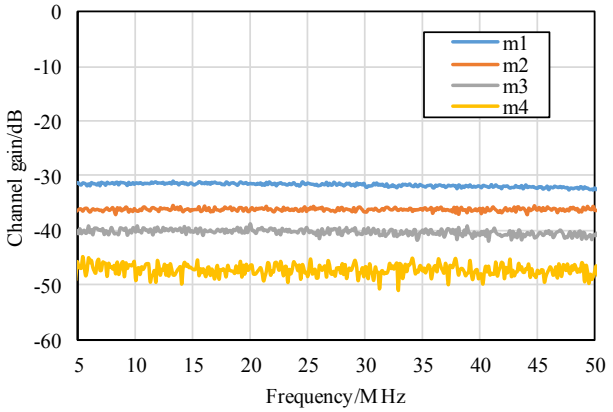

Figure 8. Measured channel gains in phantom with electrode pair distance 5cm.

The above analysis reveal that larger implant shows definitely benefits for channel gain. Provided a fixed implant length, the effective means to enhance the channel gain is to enlarge the metal electrode part, i.e., the conducting area with the human tissue.

Beside the optimally aligned electrode pairs, Figure 9 shows the gain variations when the electrode pair are displaced with 45 degree angle. Compared with alignment, 45 degree displacement corresponds to approximately 2-3 dB additional loss for m1, m2 and m3. For m4, the gain variation is relatively large not to draw a resonable conclusion, since the channel gain itself is already relatively too small. In fact, the smaller the implants (m3 and m4 vs. m1 and m2), the larger the additional loss variation. The larger the metal electrode, the smaller the additional loss (m1 vs. m2). On the other hand, when the electrode pair is vertical to each other, the transmission connection is totally lost and not any more detectable above the noise level, since the E-field is normal to the receiving interval.

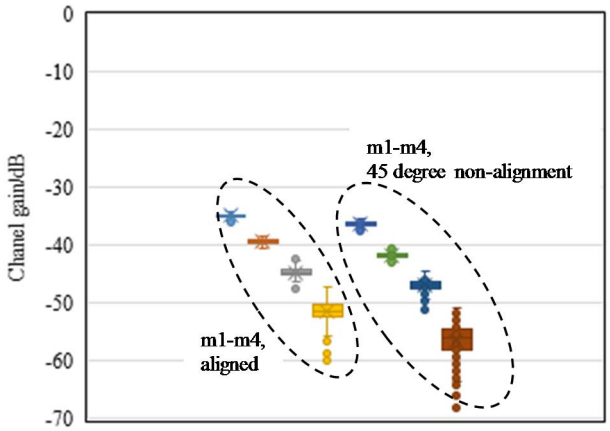

Figure 9. Measured channel gain comparison for alignment and 45 degree non-alignment, with 7 cm electrode pair distance.

3 SAR evaluation

Since the HBC electrode is touching the conductive human body tissues, it is necessary to comply with the safety guideline of SAR to ensure the human safety. Since the implanted electrode has a very small size, the induced SAR would be highly localized so that the local peak SAR will be of most interest. According to the ICNIRP safety guideline [5], a localized SAR as averaged over any ten-gram tissue should never exceed 2 W/kg for public exposure in the frequency range of 10 MHz to 10 GHz.

Figure 10 shows the numerical torso model and the calculated 10-g average SAR distribution on cross-section cut plane of the torso voxel model. The 0.2V potential port is used to excite the implanted electrode with opposite polarity. The resulting SAR is compared in Figure with that of homogeneous CAD model (with 2/3 muscle dielectric properties). The SAR results are very close to each other and they are in mW/kg, much smaller than the safety guideline 2 W/kg.

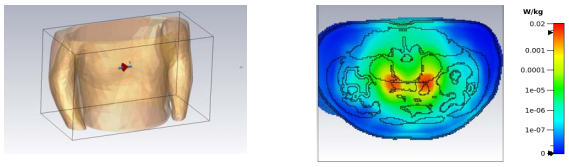

Figure 10. Numerical model (left) and 10-g SAR distribution (right) of m1 excitation at 21MHz with 0.2V potential excitation locating in muscle tissue region

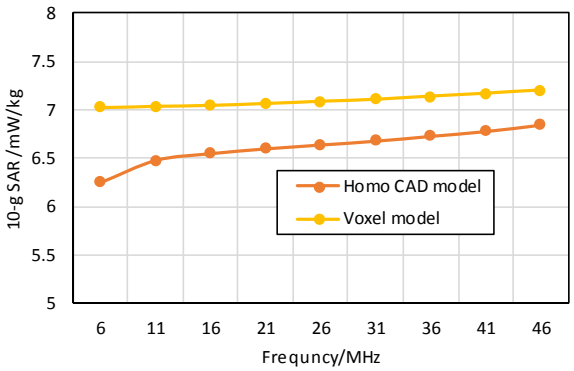

Figure 11. 10-g averaged SAR peak comparison of homogeneous CAD model and heterogeneous Voxel model with 0.2V potential excitation

Besides, peak current of 1mA is utilized as well to evaluate the resulting SAR for the four prototypes and the results are compared in Figure 10. Smaller metal electrode (m2 and m4) demonstrates higher SAR, since the resulting E-field is higher around the electrode than that of the larger electrode with the same current excitation. Moreover, the SAR is highly localized therefore the rod length make less influence on the SAR (m1 vs. m3 and m2 vs. m4).

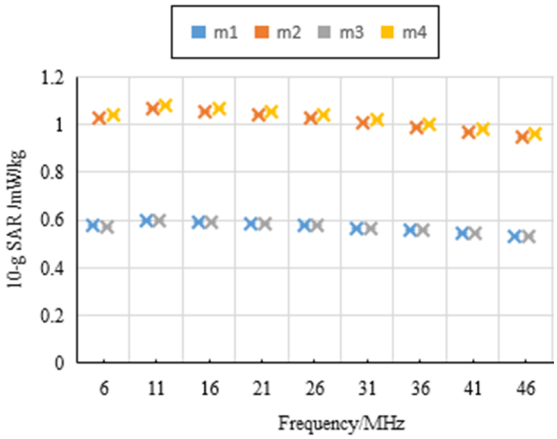

Figure 12. 10-g averaged SAR peak comparison of four electrode prototypes with 1 mA current excitation

4 References

1. J. Zhao, X. Chen et al., A Review on Human Body Communication: Signal Propagation Model, Communication Performance, and Experimental Issues, Wireless Communications and Mobile Computing, Article ID 5842310, Hindawi, 2017

2. B. Kibret, M. Seyedi, D. T. H. Lai, and M. Faulkner, "Investigation of galvanic-coupled intra body communication using the human body circuit model," IEEE J. Biomed. Health Inform., vol. 18, no. 4, pp. 1196–1206, Jul. 2014.

3. M. A. Callejón, J. Reina-Tosina, D. Naranjo-Hernández, and L. M. Roa, "Galvanic coupling transmission in intrabody communication: A finite element approach," IEEE Trans. Biomed. Eng., vol. 61, no. 3, pp. 775–783, Mar. 2014.

4. S. H. Pun, Y. M. Gao, P. Mak, M. I Vai, and M. Du, "Quasistatic modeling of human limb for intra-body communications with experiments," IEEE Trans. Inf. Technol. Biomed., vol. 15, no. 6, pp. 870–876, Nov. 2011.

5. ICNIRP, "Guidelines for limiting exposure to time-varying electric, magnetic and electromagnetic fields (up to 300 GHz)," Health Physics, Vo1.74, pp.494-522, 1998.